



# HHS Public Access

Author manuscript

*Biochemistry*. Author manuscript; available in PMC 2018 January 04.

Published in final edited form as:

*Biochemistry*. 2017 September 12; 56(36): 4747–4750. doi:10.1021/acs.biochem.7b00654.

## Mannobiose Binding Induces Changes in Hydrogen Bonding and Protonation States of Acidic Residues in Concanavalin A As Revealed by Neutron Crystallography

Oksana O. Gerlits<sup>†</sup>, Leighton Coates<sup>‡</sup>, Robert J. Woods<sup>§</sup>, and Andrey Kovalevsky<sup>\*,‡</sup>

<sup>†</sup>UT/ORNL Joint Institute for Biological Sciences, University of Tennessee, Knoxville, Tennessee 37996, United States

<sup>‡</sup>Biology and Soft Matter Division, Oak Ridge National Laboratory, Oak Ridge, Tennessee 37831, United States

<sup>§</sup>Complex Carbohydrate Research Center, University of Georgia, Athens, Georgia 30602-4712, United States

### Abstract

Plant lectins are carbohydrate-binding proteins with various biomedical applications. Concanavalin A (Con A) holds promise in treating cancerous tumors. To better understand the Con A carbohydrate binding specificity, we obtained a room-temperature neutron structure of this legume lectin in complex with a disaccharide Man $\alpha$ 1–2Man, mannobiose. The neutron structure afforded direct visualization of the hydrogen bonding between the protein and ligand, showing that the ligand is able to alter both protonation states and interactions for residues located close to and distant from the binding site. An unprecedented low-barrier hydrogen bond was observed forming between the carboxylic side chains of Asp28 and Glu8, with the D atom positioned equidistant from the oxygen atoms having an O $\cdots$ D $\cdots$ O angle of 101.5°.

### Graphical abstract

\*Corresponding Author: kovalevskyay@ornl.gov. Phone: +1 505 310 4184.

#### ORCID

Andrey Kovalevsky: 0000-0003-4459-9142

#### Author Contributions

O.O.G., L.C., R.J.W., and A.K. designed the research. O.O.G. and A.K. performed the research. O.O.G. analyzed data. O.O.G., L.C., R.J.W., and A.K. wrote the paper.

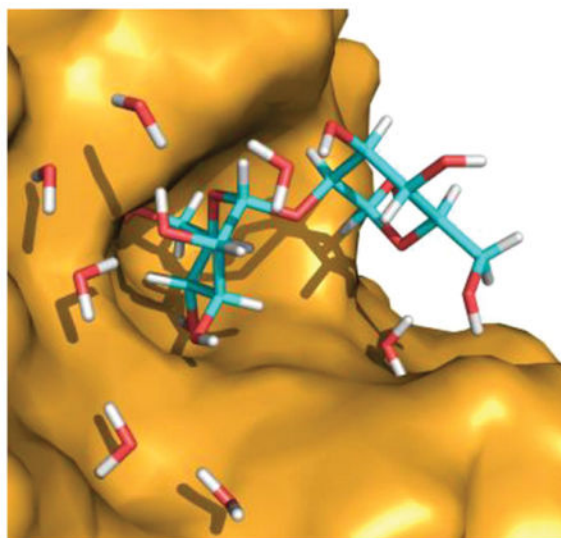
#### Notes

The authors declare no competing financial interest.

#### Supporting Information

The Supporting Information is available free of charge on the ACS Publications website at DOI: 10.1021/acs.bio-chem.7b00654.

A detailed description of crystallization methods, X-ray and neutron data collection, joint X-ray/neutron refinement, crystallographic statistics (Table S1), and Figures S1–S4 (PDF)



Plant lectins are structurally diverse carbohydrate-binding proteins, frequently employed for carbohydrate detection and capture. Lectins hold great potential for antitumor, antifungal, and antiviral therapies.<sup>1</sup> Among their many applications, lectins are used for early detection of carbohydrate-based cancer biomarkers and have anticancer activity.<sup>2</sup>

Concanavalin A (ConA) is a legume lectin extracted from jack bean seeds whose affinity for mannose/glucose depends on  $\text{Ca}^{2+}/\text{Mn}^{2+}$ . It has exhibited potential as an antitumor agent that can kill various types of human cancer cells through apoptosis, autophagy, or anti-angiogenesis.<sup>2,3</sup> Therefore, detailed structural studies of ConA in complex with carbohydrates are important for providing a deeper understanding of its specificity and may offer insights for protein engineering efforts to reduce its hepatic cytotoxicity.<sup>3</sup> Consequently, the structures of many complexes of ConA with different carbohydrates have been determined by X-ray crystallography.<sup>4-8</sup> The structures revealed details of the saccharide binding modes and changes in the water structure in the carbohydrate-binding site. Direct hydrogen bonds and water-mediated interactions were shown to play critical roles in the recognition and binding affinity of the carbohydrates bound to ConA. Hydrogen (H) atoms are the key players in such interactions but are, for the most part, invisible in X-ray crystallographic structures. Moreover, even in very high resolution X-ray structures, the electron density maps may be misleading and the placement of H atoms at specific positions can be ambiguous. This is because H, with only one electron, possesses poor X-ray scattering power, and in polar bonds (OH, NH, etc.), the effective electron density of the H atom is reduced. Thus, very acidic H atoms, and those involved in strong hydrogen bonds when an H atom is positioned halfway between two heavier atoms, are virtually impossible to reliably detect in X-ray structures. In contrast, neutrons are scattered from atomic nuclei, and the scattering power of H is similar to those of carbon, nitrogen, and oxygen. As a result, neutron crystallography can directly locate H atoms in protein structures.<sup>9</sup> Strong incoherent neutron scattering by protium ( $^1\text{H}$ ) atoms produces high background in neutron diffraction images; thus,  $^1\text{H}$  atoms are normally replaced with deuterium ( $^2\text{H}$ , termed D throughout) in protein crystals to improve the signal-to-noise ratio. H/D exchange with  $\text{D}_2\text{O}$

or full protein deuteration during expression is employed to reduce the amount of H present in crystals. Neutron crystallography is the method of choice for obtaining accurate positions of D atoms in macromolecular structures and for visualizing hydrogen bonds.<sup>10</sup> It has been demonstrated<sup>11,12</sup> that, because of the high neutron scattering power of D, which is equal in magnitude to those of C, O, and N, D atom positions can be accurately determined in neutron scattering length density maps even at resolutions as low as 2.5–2.6 Å.

Here we report a room-temperature neutron structure of H/D-exchanged ConA in complex with the known ligand Man $\alpha$ 1–2Man [mannobiose (Scheme 1 and Figure S1)] determined at 2.5 Å resolution. The neutron structure was refined jointly with a 1.8 Å resolution room-temperature X-ray data (Table S1). We discuss the details of the disaccharide binding interactions and changes in proton positions, protonation states, and water structure caused by binding of the ligand. We compare D atom positions observed in our current neutron structure with the proposed H atom locations in the high-resolution X-ray structure of the same complex.<sup>13</sup> We extend our comparison to previously determined neutron<sup>14–17</sup> and ultra-high resolution X-ray<sup>18</sup> structures of saccharide-free ConA. We note interesting changes in protonation states and hydrogen bonding that occur due to ligand binding for protein residues located both close to and distant from the carbohydrate-binding site.

Tetrameric ConA binds mannobiose at the protein surface site lined by residues 12–16, 98–100, 207, 208, and 226–228 (Figure 1 and Figures S2 and S3). The nonreducing (terminal) mannose residue (Man1 in Figure 1) makes six direct hydrogen bonds and one water-mediated interaction through W1 with ConA, whereas the reducing mannose residue (Man2) forms one direct hydrogen bond and one water-mediated contact through W2.

These interactions are similar to those detected in the 1.2 Å low-temperature structure of this complex determined previously [the two structures superimpose with a main chain root-mean-square deviation (RMSD) of 0.3 Å].<sup>13</sup> One difference is that, in the room-temperature neutron structure, the side chain of Arg228 is not disordered and does not make a hydrogen bond with O6 of Man2, similar to that observed for one of the Arg228 alternate conformations in the low-temperature X-ray structure. Instead, in the neutron structure, a chain of water molecules, acting as a hydrating shell for the mannobiose, connects the side chain of Arg228 to O3 of Man2 through O2 of Man1 (Figure 2). Structural variations in protein side chain positions and water structure have been noted before for structures obtained at 100 K and room temperature and occur due to the quick flash-freezing of crystals, which can cause a distortion in the repertoire of protein conformations.<sup>19,20</sup> The disaccharide has additional interactions with two symmetry-related molecules, which are not part of the tetramer and may not interact with mannobiose in solution. Man1 O3 makes a hydrogen bond with the carboxylic group of Asp71<sub>sym</sub>. Man2 O1 is in a tight hydrogen bond with the main chain carbonyl of Ser184<sub>sym</sub>. Interestingly, Man2 O6 donates its D in a bifurcated hydrogen bond with Asp16 and Asn118<sub>sym</sub> and in addition has a water-mediated contact with Asp71<sub>sym</sub> through a symmetry-related W3<sub>sym</sub>.

The most striking observation is that the side chain of Asp71<sub>sym</sub> is observed in the protonated (neutral), carboxylic acid, form (Figure 3). The carboxyl of Asp71<sub>sym</sub> accepts two D atoms in hydrogen bonds, whereas the O–D group makes an O–D $\cdots\pi$  interaction with

the conjugated guanidinium system of Arg228. Asp208 was instead suggested to be protonated in the low-temperature X-ray structure of this complex,<sup>13</sup> donating its H in a hydrogen bond with a metal-coordinated water molecule. We do not observe a D on Asp208 in the room-temperature neutron structure, where the carboxylate accepts a D atom from the metal-coordinated D<sub>2</sub>O. It should be noted that the 1.2 Å resolution of the published X-ray structure is not high enough to detect H atoms, because the standard OH bond length of 0.95 Å is significantly shorter than the resolution of the structure. The neutron structure even at 2.5 Å resolution is more reliable for the direct visualization of hydrogen atoms.<sup>9</sup>

It is also instructive to compare the current neutron structure of the ConA–mannobiose complex with the structures of apo ConA obtained via both X-ray and neutron crystallography,<sup>14–18</sup> because ligand binding can modulate protonation states and hydrogen bonding for the functional groups for the protein and ligand.<sup>21,22</sup> Several neutron structures have been obtained for apo ConA, both at room temperature<sup>14,15,17</sup> and at 15 K.<sup>16</sup> Ahmed et al.<sup>17</sup> reported protonation of Asp82 in the highest-resolution neutron structure at 2.2 Å at room temperature, whereas no protonation of Asp or Glu residues was reported in the other published neutron structures, which could be a result of the poorer quality of data for those earlier neutron crystallographic experiments. Importantly, Asp82 was also suggested to exist in the protonated form in apo ConA based on the ultra-high-resolution (0.94 Å) X-ray structure obtained at 100 K, in addition to residues Asp28, Asp136, and Glu102.<sup>18</sup> Although H atoms were not directly visible on these carboxylic groups, their protonation states were derived on the basis of the unrestrained refinement of C–O distances. However, protonation of only Asp82 was convincingly observed in the 2.2 Å neutron structure,<sup>17</sup> with possible protonation of Asp28, which is a special case to be discussed below. It must be noted, therefore, that the unrestrained refinement of C–O bond lengths for carboxylic groups may not reliably inform on the protonation state of this chemical group even at ultrahigh resolution. In the current neutron structure of the ConA–mannobiose complex, Asp82 is not protonated, whereas Asp71 is. Therefore, binding of the disaccharide probably induces a change in the protonation state of a carboxylic group (Asp71<sub>sym</sub>) that is in direct contact with the ligand, while also leading to the deprotonation of another carboxylic group (Asp82) located distal to the binding site.

The protonation state of Asp28 is of particular interest, because it is positioned within hydrogen bonding distance of the Glu8 side chain, which is coordinated to a Mn<sup>2+</sup> ion. The Asp28–Glu8 feature is reminiscent of an Asp–Glu pair in the active site of the glycoside hydrolase lysozyme and has been suggested as a possible latent catalytic site.<sup>14,18</sup> No lectins are known to have enzymatic activity, but the proximity of these two residues is conserved in other proteins of the legume lectin family, suggesting a possible functional evolutionary relationship between some lectins and glycoside hydrolases. Asp28 was suggested to be protonated in the 0.94 Å X-ray structure,<sup>18</sup> while its protonation was less clear in the 2.2 Å neutron structure. In the earlier neutron structure of apo ConA,<sup>14</sup> the hydrogen on Asp28 was observed, indicating its protonation, but it did not exchange with D. This peculiar behavior of the H atom located on the side chain of a protein surface residue was noted as evidence of the inability of ConA to have any enzymatic activity. However, Habash et al.<sup>14</sup> suggested that, if the Asp28 proton exchanged with D, it could become available to participate in the hydrolase activity.

When mannobiose binds to ConA, the nature of the hydrogen bond between Asp28 and Glu8 changes, with the proton no longer belonging to just the Asp28 side chain. In the neutron structure of this complex, a D atom is observed positioned equidistant from the two oxygen atoms of the carboxylic groups taking part in a possible low-barrier hydrogen bond (Figure 4). In a low-barrier hydrogen bond, the zero-point energy is close to the height of the energy barrier that has to be overcome to transfer a proton between the two oxygen atoms, and the highest probability for the proton position is exactly at the center with equal distances to the oxygens.<sup>23,24</sup> The D $\cdots$ O distances are essentially equal: 1.5 Å for D $\cdots$ O $\epsilon$ 1(Glu8) and 1.6 Å for D $\cdots$ O $\delta$ 2(Asp28). The heavy-atom O $\delta$ 2(Asp28) $\cdots$ O $\epsilon$ 1(Glu8) distance has decreased slightly to 2.4 Å in the ConA–mannobiose complex compared to 2.6 Å in the apo ConA room-temperature neutron structure. Moreover, the D atom is not located on the line connecting O $\delta$ 2(Asp28) and O $\epsilon$ 1(Glu8) atoms but is directed to the side, with an O $\delta$ 2(Asp28) $\cdots$ D $\cdots$ O $\epsilon$ 1(Glu8) angle of 101.5°. Such a geometry of the hydrogen bond can be explained by the non-coplanarity of the Asp28 and Glu8 carboxylate groups. The two COO moieties are rotated relative to each other by 67°; thus, the lone electron pairs involved in the hydrogen bond do not face each other. Consequently, the D atom location is governed by the juxtaposition of the lone pairs, allowing the formation of a strong hydrogen bond. The D atom also is only slightly out of the COO planes, with D–O–C–O dihedral angles of 34° and 167° for Asp28 and Glu8, respectively. To the best of our knowledge, this is the first observation of such a hydrogen bond geometry in a protein. Importantly, a hydrogen atom participating in such a low-barrier hydrogen bond would not be visible in an X-ray structure, because at the location of its highest nuclear probability it possesses virtually no electron density.

Binding of mannobiose does not substantially disturb the sugar-binding site of ConA. When the room-temperature structures of the ConA–mannobiose complex and apo ConA<sup>17</sup> are superimposed, there is very little change in the main chain of the protein [RMSD of 0.5 Å for the main chain atoms (Figure S4)]. The most significant effect is observed for the main chain atoms of Asp16 and Leu99, each moving ~1 Å toward the disaccharide to form hydrogen bonds and hydrophobic interactions with the ligand. Only the positions of the side chains are altered for other residues. For instance, in the ConA–mannobiose complex, Tyr100 and Arg228 both shift away from their respective positions in the apo ConA structure to prevent steric clashes. Changes in the positions of Tyr12 and Asn14, on the other hand, are very small. Thus, it appears that the binding site in ConA is already preformed before the disaccharide binds, and ligand binding mainly induces small alterations in the positions of side chains of proximal amino acid residues.

In conclusion, we have demonstrated that a disaccharide binding to its target lectin can induce protonation state changes of the residues located in the binding site and distant from it. The origin of these changes remains to be studied theoretically. A recent study reported a neutron structure of the carbohydrate binding module of Xyn10 xylanase bound to an oligosaccharide;<sup>25</sup> however, the lack of an apo structure precluded discussion of structural changes due to ligand binding. Binding of mannobiose to ConA also changes a normal hydrogen bond between Asp28 and Glu8 into a possible low-barrier hydrogen bond, with the D atom observed equidistant from the carboxylic groups of these residues. The mutual orientation of the Asp28 and Glu8 side chains leads to distortion in the position of the D

atom away from a straight line connecting the two oxygens, which is an unprecedented observation that would not be possible to observe with X-rays. We thus stress the uniqueness of neutron diffraction, which is capable of direct visualization of nuclear positions even for hydrogen atoms with little or no electron density (i.e., H<sup>+</sup>).

## Supplementary Material

Refer to Web version on PubMed Central for supplementary material.

## Acknowledgments

### Funding

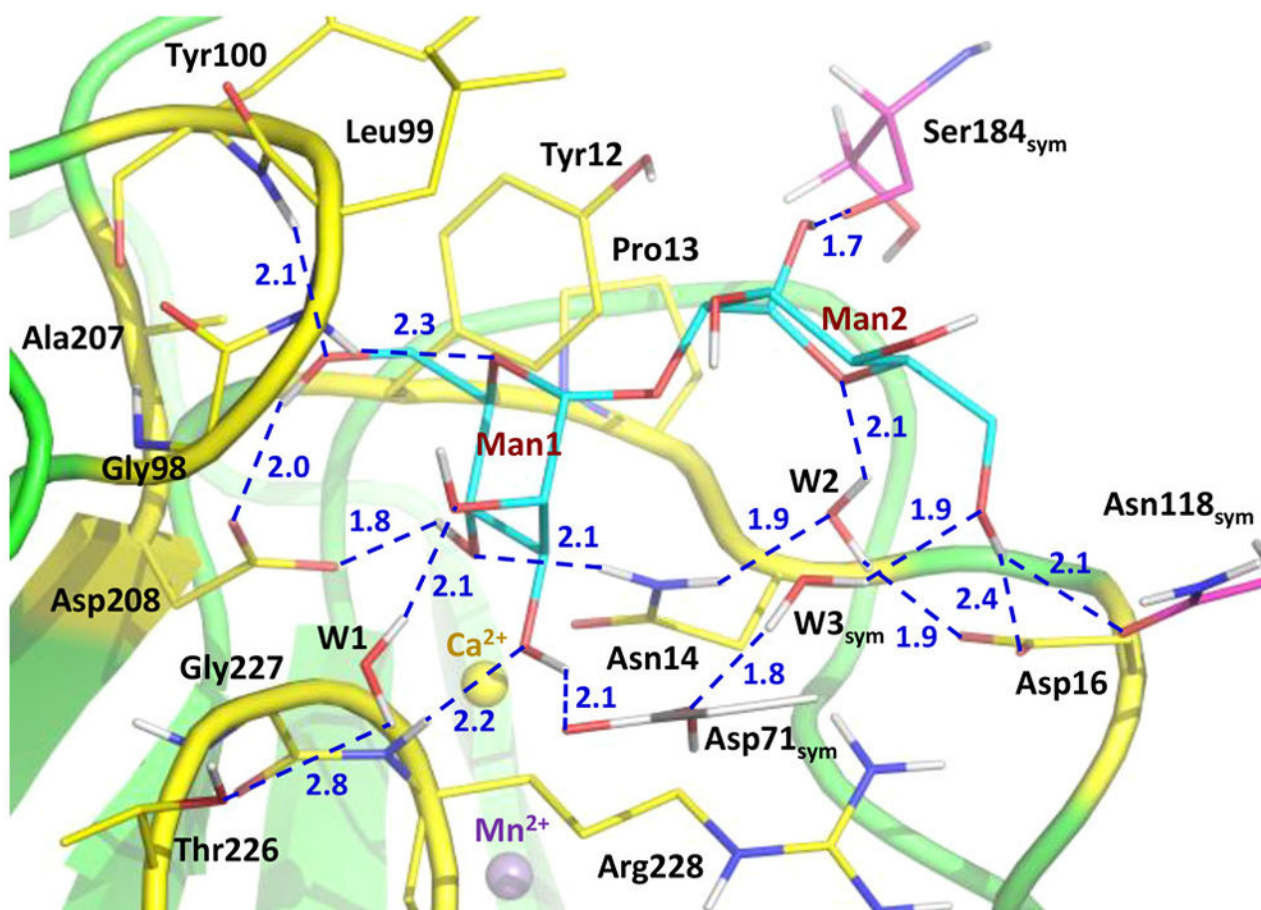
The research at Oak Ridge National Laboratory's (ORNL's) Spallation Neutron Source and High Flux Isotope Reactor was sponsored by the Scientific User Facilities Division, Office of Basic Energy Sciences, U.S. Department of Energy (US DOE). The Office of Biological and Environmental Research supported research at ORNL's Center for Structural Molecular Biology (CSMB), using facilities supported by the Scientific User Facilities Division, Office of Basic Energy Sciences, US DOE. IMAGINE instrument operations are supported by the Office of Basic Energy Sciences, US DOE. This paper has been authored by UT-Battelle LLC under DOE Contract DE-AC05-00OR22725.

## References

1. Van Damme EJM, Peumans WJ, Barre A, Rouge P. *Crit Rev Plant Sci*. 1998; 17:575–692.
2. Yau T, Dan X, Ng CCW, Ng TB. *Molecules*. 2015; 20:3791–3810. [PubMed: 25730388]
3. Li WW, Yu JY, Xu HL, Bao JK. *Biochem Biophys Res Commun*. 2011; 414:282–286. [PubMed: 21951850]
4. Francois-Heude M, Mendez-Ardoy A, Cendret V, Lafite P, Daniellou R, Ortiz Mellet C, Garcia Fernandez JM, Moreau V, Djedaini-Pilard F. *Chem - Eur J*. 2015; 21:1978–1991. [PubMed: 25483029]
5. Kadirvelraj R, Foley BL, Dyekjaer JD, Woods RJ. *J Am Chem Soc*. 2008; 130:16933–16942. [PubMed: 19053475]
6. Hamodrakas SJ, Kanellopoulos PN, Pavlou K, Tucker PA. *J Struct Biol*. 1997; 118:23–30. [PubMed: 9087912]
7. Moothoo DN, Canan B, Field RA, Naismith JH. *Glycobiology*. 1999; 9:539–545. [PubMed: 10336986]
8. Naismith JH, Field RA. *J Biol Chem*. 1996; 271:972–976. [PubMed: 8557713]
9. Blakeley MP, Hasnain SS, Antonyuk SV. *IUCrJ*. 2015; 2:464–474.
10. Blakeley MP. *Crystallogr Rev*. 2009; 15:157–218.
11. Banco MT, Mishra V, Ostermann A, Schrader TE, Evans GB, Kovalevsky AY, Ronning DR. *Proc Natl Acad Sci U S A*. 2016; 113:13756–13761. [PubMed: 27856757]
12. Langan PS, Close DW, Coates L, Rocha RC, Ghosh K, Kiss C, Waldo G, Freyer J, Kovalevsky A, Bradbury ARM. *J Mol Biol*. 2016; 428:1776–1789. [PubMed: 27000644]
13. Sanders DAR, Moothoo DN, Raftery J, Howard AJ, Helliwell JR, Naismith JH. *J Mol Biol*. 2001; 310:875–884. [PubMed: 11453694]
14. Habash J, Raftery J, Weisgerber S, Cassetta A, Lehmann MS, Høghøj P, Wilkinson C, Campbell JW, Helliwell JR. *J Chem Soc, Faraday Trans*. 1997; 93:4313–4317.
15. Habash J, Raftery J, Nuttall R, Price HJ, Wilkinson C, Kalb (Gilboa) AJ, Helliwell JR. *Acta Crystallogr Sect D: Biol Crystallogr*. 2000; 56:541–550. [PubMed: 10771422]
16. Blakeley MP, Kalb (Gilboa) AJ, Helliwell JR, Myles DAA. *Proc Natl Acad Sci U S A*. 2004; 101:16405–16410. [PubMed: 15525703]
17. Ahmed HU, Blakeley MP, Cianci M, Cruickshank DWJ, Hubbard JA, Helliwell JR. *Acta Crystallogr Sect D: Biol Crystallogr*. 2007; 63:906–922. [PubMed: 17642517]

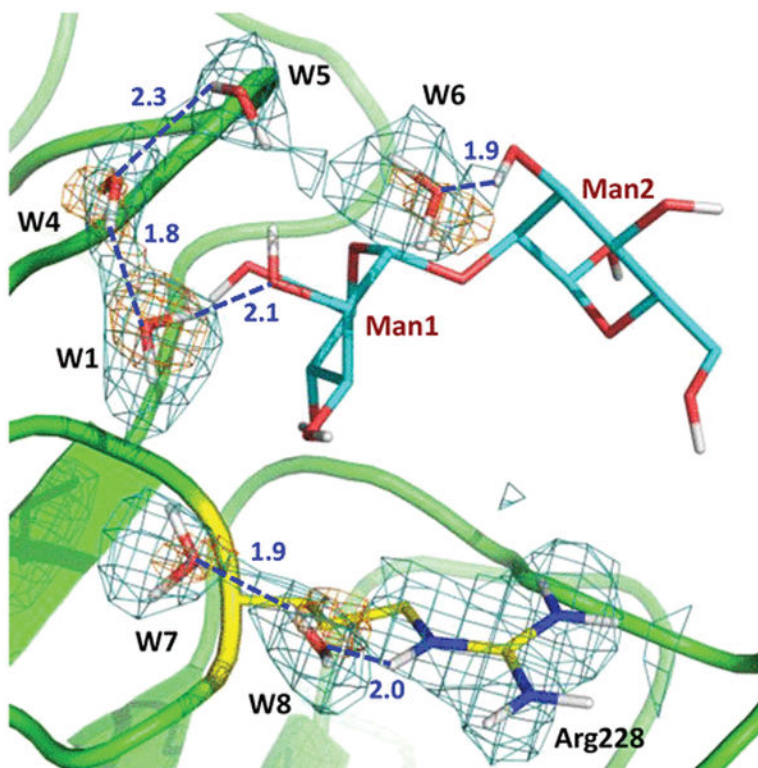


18. Deacon A, Gleichmann T, Kalb (Gilboa) AJ, Price H, Raftery J, Bradbrook G, Yariv J, Helliwell JR. *J Chem Soc, Faraday Trans.* 1997; 93:4305–4312.
19. Fraser JS, van den Bedem H, Samelson AJ, Lang PT, Holton JM, Echols N, Alber T. *Proc Natl Acad Sci U S A.* 2011; 108:16247–16252. [PubMed: 21918110]
20. Keedy DA, van den Bedem H, Sivak DA, Petsko GA, Ringe D, Wilson MA, Fraser JS. *Structure.* 2014; 22:899–910. [PubMed: 24882744]
21. Niimura N, Takimoto-Kamimura M, Tanaka I. *Encyclopedia of Analytical Chemistry.* 2016:1–30.
22. Schiebel J, Gaspari R, Sandner A, Ngo K, Gerber HD, Cavalli A, Ostermann A, Heine A, Klebe G. *Angew Chem, Int Ed.* 2017; 56:4887–4890.
23. Perrin CL, Nielson JB. *Annu Rev Phys Chem.* 1997; 48:511–544. [PubMed: 9348662]
24. Grabowski SJ. *Annu Rep Prog Chem, Sect C: Phys Chem.* 2006; 102:131–165.
25. Fisher SZ, von Schantz L, Hakansson M, Logan DR, Ohlin M. *Biochemistry.* 2015; 54:6435–6438. [PubMed: 26451738]

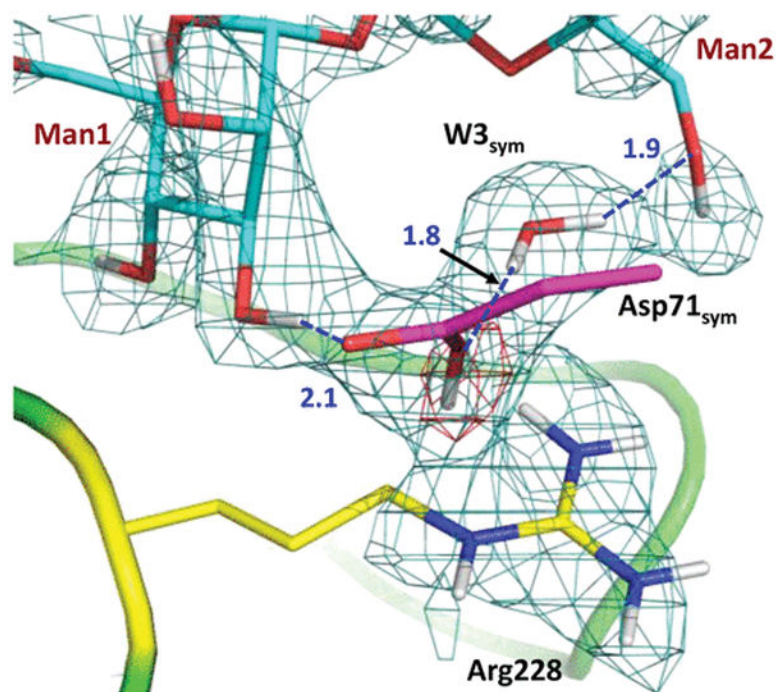


**Figure 1.** Hydrogen bonding and water-mediated interactions made by mannobiose with ConA residues. Carbohydrate-binding site residues are color-coded with carbons colored yellow. The residues from the two symmetry-related ConA molecules are color-coded with carbons colored gray and magenta. D···O and D···N distances are shown as blue dashed lines and are given in units of angstroms.

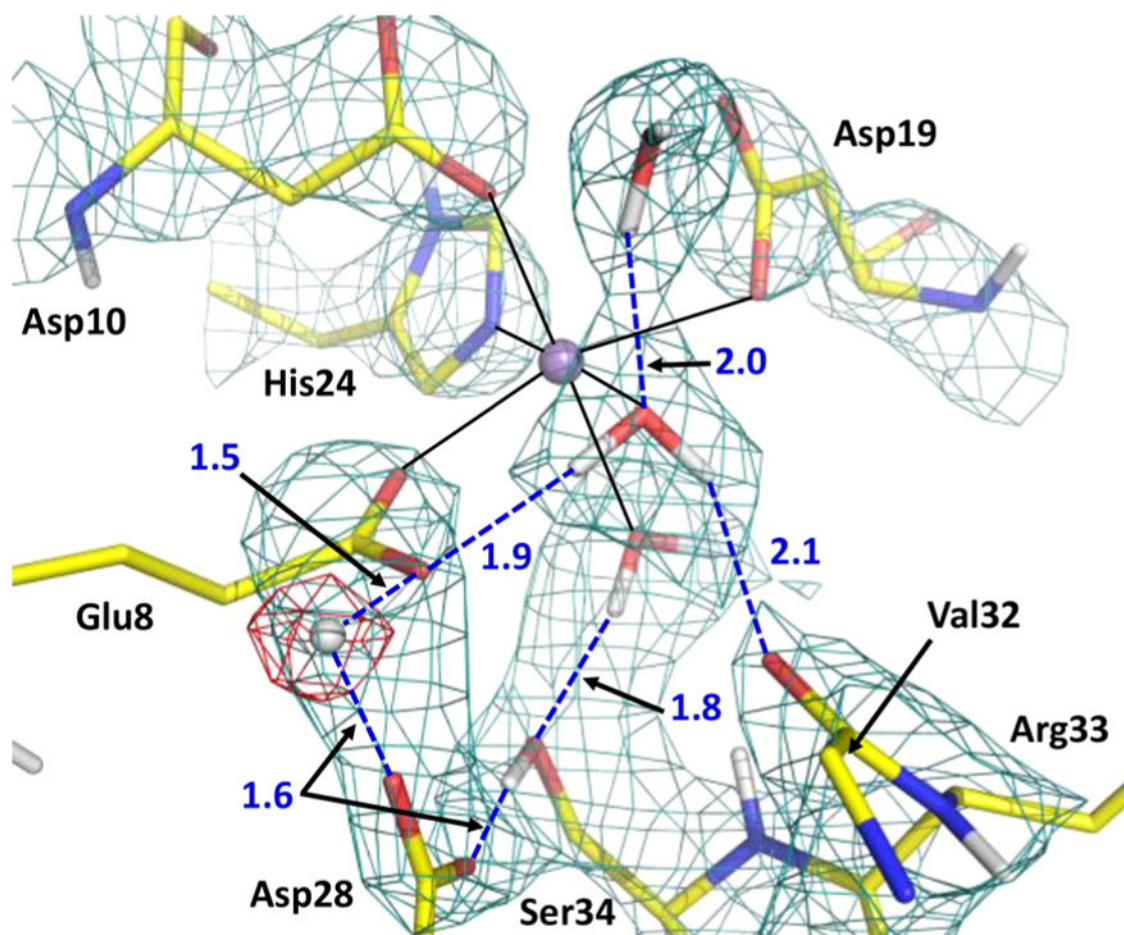




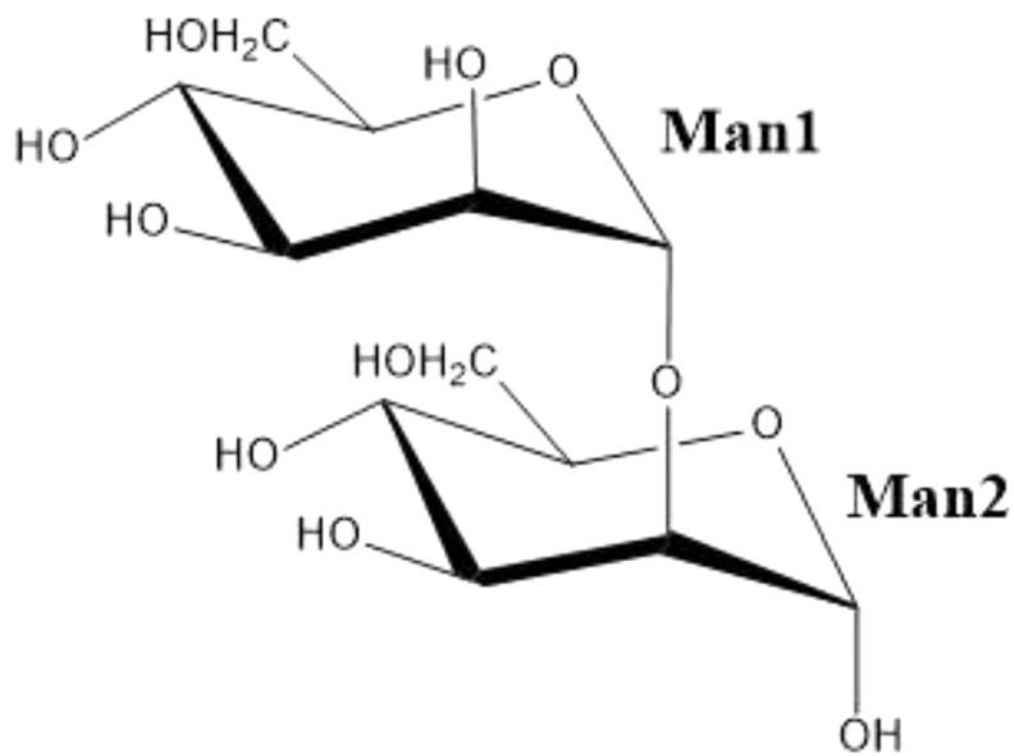
**Figure 2.** Water chain hydrating mannobiose spans a curve from Arg228 to O3 of Man2. The  $2F_O - F_C$  neutron scattering length density map (teal mesh) and the  $2F_O - F_C$  electron density map (orange mesh) for water molecules are both shown at  $1.2\sigma$  contour levels. Hydrogen bonds are shown as blue dashed lines, and D $\cdots$ O distances are given in units of angstroms. W1 is the same water as shown in Figure 1 (for the sake of clarity, W2 and W3<sub>sym</sub> were omitted).



**Figure 3.** Interactions between the protonated Asp71<sub>sym</sub> from the symmetry-related ConA and mannobiose. The  $2F_O - F_C$  neutron scattering length density map (teal mesh) is shown at the  $1.2\sigma$  contour level. The omit difference  $F_O - F_C$  neutron scattering length density map (red mesh) for the carboxyl D atom is shown at the  $3\sigma$  contour level. Hydrogen bonds are shown as blue dashed lines, and D $\cdots$ O distances are given in units of angstroms.



**Figure 4.**  $\text{Mn}^{2+}$  (violet sphere)-binding site and protonation of the Asp28–Glu8 pair. The  $2F_{\text{O}} - F_{\text{C}}$  neutron scattering length density map (teal mesh) is shown at the  $1.5\sigma$  contour level. The omit difference  $F_{\text{O}} - F_{\text{C}}$  neutron scattering length density map (red mesh) for the D atom in the low-barrier hydrogen bond is shown at the  $3\sigma$  contour level. Hydrogen bonds are shown as blue dashed lines, and D $\cdots$ O distances are given in units of angstroms. The side chain of Val32 was omitted for the sake of clarity.



**Scheme 1.**  
Chemical Structure of Man $\alpha$ 1-2Man